Regular Article

PHYSICAL CHEMISTRY RESEARCH
Published by the
Iranian Chemical Society
www.physchemres.org
info@physchemres.org

Phys. Chem. Res., Vol. 11, No. 1, 23-31, March 2023
DOI: 10.22036/PCR.2022.333784.2050

Enhanced Luminescence and Energy Transfer of Bi^{3+}/Dy^{3+} Co-doped $La_2Zr_2O_7$ Nanophosphors for pc-LED Applications

B.V. Naveen Kumar[a,b], Y. Nirmal Rajeev[a,c], Esub Basha Shaik[d], K. Venkatarao[a,e], K. Ramachandra Rao[d] and Sandhya Cole[a,*]

[a]*Department of Physics, Acharya Nagarjuna Univeristy, Guntur-522510,A.P, India*
[b]*Department of Physics, Shri Vishnu Engineering College for Women (A), Bhimavaram-534202, A.P, India*
[c]*Department of Physics, V.R.Siddhartha Engineering College (A), Kanuru, Vijayawada-520007, A.P. India*
[d]*Crystal Growth & Nanoscience Research Center, Government College (A), Rajahmundry- 533105, A.P, India*
[e]*Department of Physics, Government Institute of Textile Technology, Guntur-522005, A.P., India*
(Received 5 March 2022, Accepted 14 April 2022)

In this study, lanthanum zirconate ($La_2Zr_2O_7$) doped with Bi^{3+} and co-doped with Dy^{3+} ions were synthesized by polyol method and their luminescence properties were reported. From XRD results, a pure cubic phase with the $Fd\bar{3}m$ space group (#227) was confirmed for the as-prepared samples. In order to understand the absorption properties and estimate the optical energy band gap values of the as-prepared samples absorption studied were used. The morphological studies of the as-prepared samples showed irregular shaped agglomerates with particle size between 60 and 90 nm. The PL emission spectra of the Bi^{3+} doped $La_2Zr_2O_7$ showed the emission of blue colour located at 460 nm ($^3P_1 \rightarrow {}^1S_0$ transition) when excited at 330 nm. The Bi^{3+} and Dy^{3+} co-doped samples exhibited the PL emission peaks around 480 nm ($^4F_{9/2} \rightarrow {}^6H_{15/2}$) and 575 nm ($^4F_{9/2} \rightarrow {}^6H_{13/2}$) when excited at 307 nm. From PL studies, the identified optimized composition was $La_2Zr_2O_7$: 0.5 at% Bi^{3+}; 2 at% Dy^{3+} with strong tunable blue-yellow emissions. The co-doping of Dy^{3+} with Bi^{3+} in the host lattice is a promising method to enhance the emission intensities for use in pc-LED.

Keywords: Emissions Spectra, Excitation, Photoluminescence, Energy-transfer, pc-LED

INTRODUCTION

Due to the importance of single-phase white luminescent materials in powder converted Light Emitting Diodes (pc-LEDs) and field emission display applications, many efforts have been made to develop these materials [1-5]. In this context, the pyrochlore structured compound $La_2Zr_2O_7$ has attracted the attention of researchers due to its unique structural and intriguing luminescent properties for various solid state lighting applications [6]. By changing temperature, pressure, and chemical doping, these ordered pyrochlore ($La_2Zr_2O_7$) undergo phase transitions to disordered fluorite of the $Fd\bar{3}m$ space group or *vice versa* [7-9]. Rare-earth (RE^{3+}) activator ions have received a lot of attention due to their good photoluminescence performance in the visible and near-infrared regions [10-13]. In particular, the emission lines of Dy^{3+} activator ions which lie under the blue and yellow regions make the phosphors much suitable for developing the white light emissions. However, emissions from Dy^{3+} ions activated phosphor have relatively low luminescent efficiency. Hence, energy transfer from sensitizers to activators is an efficient way to improve the luminescent efficiency and intensity of the activator ion.

When the Dy^{3+} ions (activator) are embedded in inorganic host materials, co-doping with Bi^{3+} ions (sensitizer) can increase their luminescent efficiency [5,14] . Since Bi^{3+} ions emit broad wavelength (its maximum

*Corresponding author. E-mail: sandhya.cole@gmail.com

peaking varies between the blue and green), the outer $6s^2$ electronic configurations of Bi^{3+} is strongly dependent on the environmental conditions such as site symmetry, coordination number, and covalence. The transitions from $^1S_0$ (ground state) to $^3P_1$ and $^1P_1$ (excited states) have an acceptable absorption capacity (UV absorption), which may increase the emission efficiency of the activator ion by exploiting the effective energy transfer (from sensitizer to activator) [15,16]. In order to have energy transfer, overlapping of the emission of sensitizer and excitation of the activator are the crucial requirements. In the present study, synthesis and characterization of Bi^{3+}/Dy^{3+} co-doped $La_2Zr_2O_7$ phosphor powders by polyol method were studied and their photoluminescence properties were evaluated. Enhanced emission and improved colour quality of the prepared samples indicated that they are suitable compounds for use in pc-LEDs.

EXPERIMENTAL

The samples of undoped, Bi^{3+}-doped and Bi^{3+}/Dy^{3+} co-doped $La_2Zr_2O_7$ nanophosphors were prepared by a simple wet-chemical method namely polyol method. The precursors employed for the synthesis are shown in Table 1.

Stoichiometric amounts of the above materials were weighed and well mixed in a round bottom flask containing 20 ml of ethylene glycol (EG), kept on hot magnetic stirrer which acts as a reducing and capping agent. To get the precipitation, 2 g of Urea was added to the above mixture and stirred well; simultaneously, the temperature of the solution was kept constant between 120-130 °C for two hours. The produced solution then was washed thrice with methanol, collected, centrifuged and dried over-night in a dust-free environment. Later, the dried samples were calcinated at 1300 °C in a furnace and were collected by grounding them in an agate mortar. The crystallinity, surface morphologies, photoluminescence, and the life-time decay analysis were carried out at room temperature using Rigaku Miniflex 300/600 (40 kV, CuK_α, 0.02° step) for X-Ray Diffraction (XRD), FEI Thermo Fisher Quanta 200F for Field Emission-Scanning Electron Microscopy (FE-SEM), and Edinburgh FLSP 920 (450W Xe lamp) for Photoluminescence (PL) studies.

Table 1. Starting Chemicals Used in Synthesis

Chemical name	Chemical formula	Purity	Chemical manufacturer
Lanthanum nitrate	$La(NO_3)_3.6H_2O$	99.99%	Sigma-Aldrich
Zirconyl nitrate	$Zr(NO_3)_3.6H_2O$	99.99%	Sigma-Aldrich
Bismuth nitrate	$Bi(NO_3)_3.5H_2O$	99.99%	Sigma-Aldrich
Dysprosium nitrate	$Dy(NO_3)_3.6H_2O$	99.99%	Sigma-Aldrich

RESULTS AND DISCUSSION

Phase Formation and Morphology

The XRD reports of undoped and $La_2Zr_2O_7$: 0.5 at.% Bi^{3+} and $La_2Zr_2O_7$: 0.5 at.% Bi^{3+}; 2 at.% Dy^{3+} phosphors annealed at 1300 °C were recorded and are shown in Fig. 1. All X-ray diffraction patterns are indexed to pure cubical phase (JCPDS No.01-071-2363) with $Fd\bar{3}m$ space group (#227) and there was no formation of impurity phases [17].Using POWDERX software, the lattice parameters of the synthesized nanophosphors were calculated that are shown in Table 2.

The calculated crystallite sizes of all samples using the Scherrer's equation were about 20 nm. The SEM image of the $La_2Zr_2O_7$: 0.5 at.% Bi^{3+}; 2 at.% Dy^{3+}phosphor is shown in Fig. 2. From the SEM image, it was found that the sample powder had irregular shaped agglomerates. By employing ImageJ software, the grain size of the agglomerates through histograms was found around 80 nm.

UV-Vis Absorption Studies of Bi^{3+}/Dy^{3+} Co-Doped $La_2Zr_2O_7$ Nanophosphors

The UV-Vis Spectrophotometer (LAB INDIA UV 3092) was used to record the UV-Vis absorbance of the as-prepared nanophosphors. The optical energy band gap of the prepared samples was measured by uniformly dissolving the particles in solvent (ethylene glycol) at the wavelength range of 190-900 nm. The UV-Vis Absorption spectra and estimated optical energy bandgap values of the $La_2Zr_2O_7$:

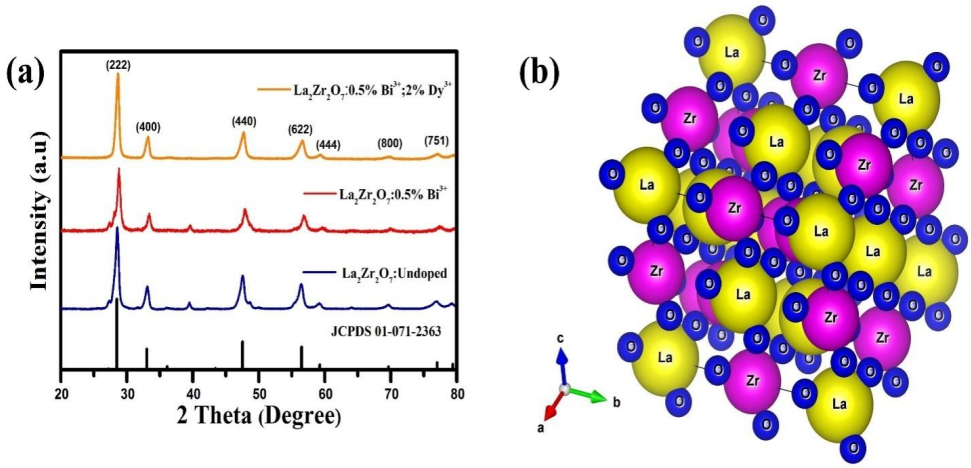

Fig. 1. (a) XRD patterns corresponding to Undoped, Bi^{3+}/Dy^{3+} Co-doped $La_2Zr_2O_7$ nanophosphors and (b) Simulated 3-D View of $La_2Zr_2O_7$ nanophosphors.

Table 2. Unit Cell Parameters of Bi^{3+}/Dy^{3+} Co-doped $La_2Zr_2O_7$ Nanophosphors

Composition	a (Å)	b (Å)	c (Å)	V $(Å)^3$
$La_2Zr_2O_7$: Undoped	10.8090	10.8090	10.8090	1262.8639
$La_2Zr_2O_7$: 0.5 at.% Bi^{3+}	10.8080	10.8080	10.8080	1262.5134
$La_2Zr_2O_7$: 0.5 at. % Bi^{3+}; 2 at. % Dy^{3+}	10.7860	10.7860	10.7860	1254.8194

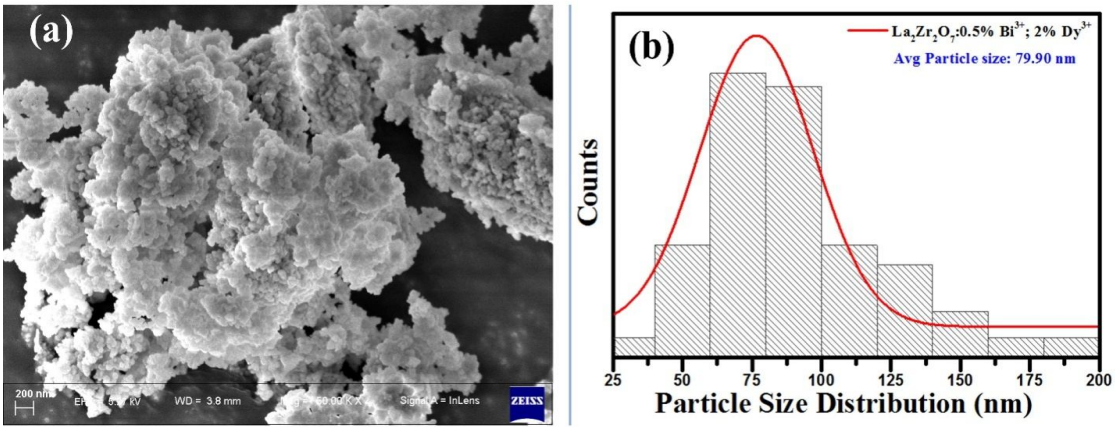

Fig. 2. (a) SEM image and (b) particle size histogram of Bi^{3+}/Dy^{3+} Co-doped $La_2Zr_2O_7$ nanophosphors.

0.5 at.% Bi^{3+} and $La_2Zr_2O_7$: 0.5 at.% Bi^{3+}; 2 at.% Dy^{3+} nanophosphors are shown in Figs. 3a and b.

The UV-Vis spectrum (Fig. 3a) shows the strongest and most noticeable absorption zone in the range of 260-275 nm. A plot of $(\alpha h\nu)^2$ *vs.* $h\nu$ was generated and examined to find the optical bandgap of the as-prepared

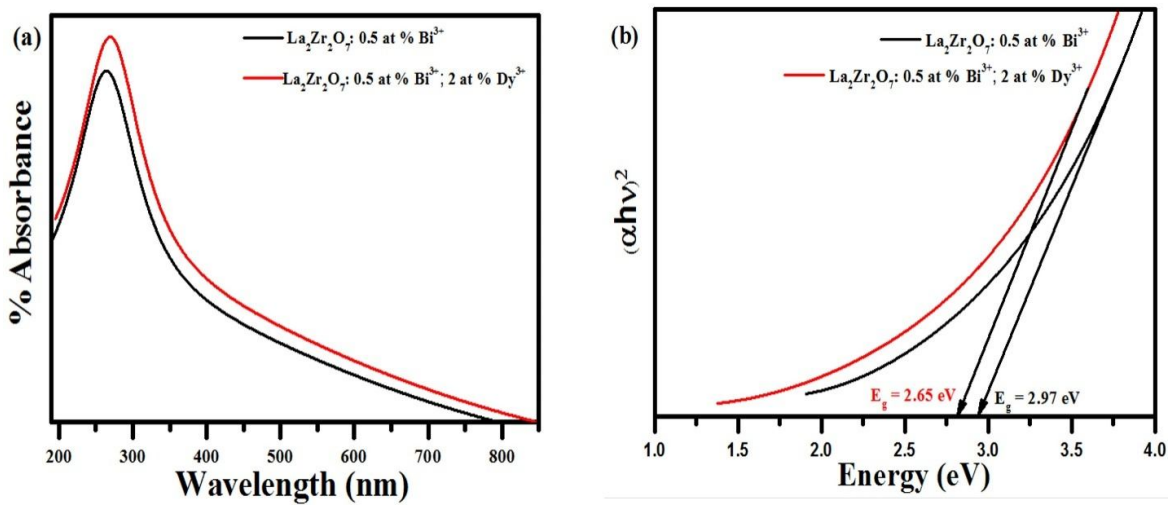

Fig. 3. (a) UV-Vis spectra and (b) optical energy bandgaps of Bi^{3+}/Dy^{3+} Co-doped $La_2Zr_2O_7$ nanophosphors.

nanophosphors. Here, α is the optical absorption coefficient and hν is the incident photon energy. The optical energy bandgap values (Fig. 3b) of the $La_2Zr_2O_7$: 0.5 at.% Bi^{3+} and $La_2Zr_2O_7$: 0.5 at.% Bi^{3+}; 2 at.% Dy^{3+} nanophosphors were 2.97 eV, and 2.65 eV, respectively, extrapolated from the linear side of the curve $(\alpha h\nu)^2 = 0$ [18]. The incorporation of the dopants into the host lattice influenced the electronic structure, resulting in the formation of intermediate energy levels, which may be responsible for the reduction in bandgap of the doped and co-doped nanophosphors [19-21].

Photoluminescence Properties of Singly Doped $La_2Zr_2O_7$: x % Bi^{3+} Phosphors

Figure 4 depicts emission (a) and excitation (b) spectra of the singly-doped $La_2Zr_2O_7$: x% Bi^{3+} (x = 0.1, 0.5, 1 & 1.5). The emission spectra of the Bi^{3+} ions doped samples at 460 nm (blue) revealed a broad peak maximum, which can be attributed to the transition $^3P_1 \rightarrow {}^1S_0$ of the Bi^{3+} ions excited at 310 nm [22]. The life-time decay curves of the Bi^{3+} ions doped samples are also represented in Fig. 4d. With an increase in the concentration of the Bi^{3+} ion, the emission intensity at 460 nm initially grew, reached to a maximum value for 0.5 at. % Bi^{3+} ions, and then declined by a further increase in concentration; this can be attributed to the concentration limiting effect. The latter was confirmed by estimating the Bi-exponential life-time values of the $La_2Zr_2O_7$:Bi^{3+} (0.1, 0.5, 1, & 1.5 at.%), which were 5.31, 7.65, 3.22, and 2.14 µs. The graphs of the relative emission intensities of Bi^{3+} ions as a function of dopant concentration are shown in Fig. 4c.

Photoluminescence Properties of Bi^{3+}/Dy^{3+} co-doped $La_2Zr_2O_7$ Phosphors

Figure 5 shows the emission spectra (a) and the excitation spectra (b) of the $La_2Zr_2O_7$: 0.5 at.% Bi^{3+}; Dy^{3+} (1, 2, 3, & 4 at.%) samples. At the excitation wavelength of 330 nm, the recorded emission spectra of the $La_2Zr_2O_7$: 0.5 at.% Bi^{3+}; Dy^{3+} (1, 2, 3, 4 at %) was consisted of blue & yellow emission lines originated from Bi^{3+} ions (blue) and Dy^{3+} ions (blue & yellow). By keeping the concentration of Bi^{3+} ions constant at 0.5 at.%, and by varying the concentration of Dy^{3+} ions as 1, 2, 3, 4 at.%, the emission intensity of the Bi^{3+} remarkably decreased. The emission intensity of the Dy^{3+} ions increased and reached a maximum for the 2 at.% concentration; further increase in concentration led to a decrease in the emission intensity. This effect can be interpreted as concentration quenching effect caused by Dy^{3+} ions energy transition and cross relaxation. The Photoluminescence intensity drops during the cross-relaxation process due to exchange interaction, radiation reabsorption, or multipole-multipole interactions in the synthesized composition [23].

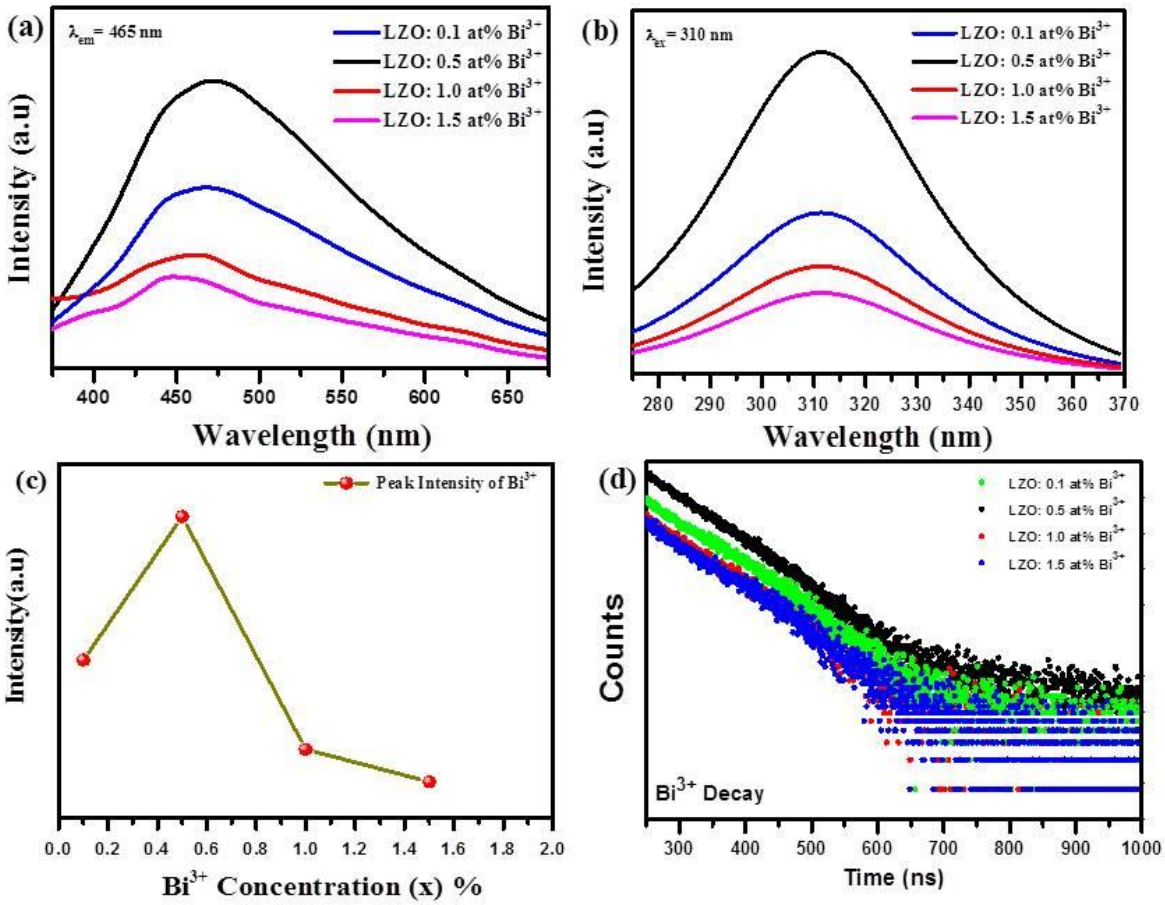

Fig. 4. Photoluminescence of Bi^{3+} doped $La_2Zr_2O_7$ nanophosphors (a) Emission (λ_{ex} = 330nm), (b) Excitation (λ_{em} = 430 nm), (c) Concentration *vs*. Intensity and (d) Lifetime decay curves.

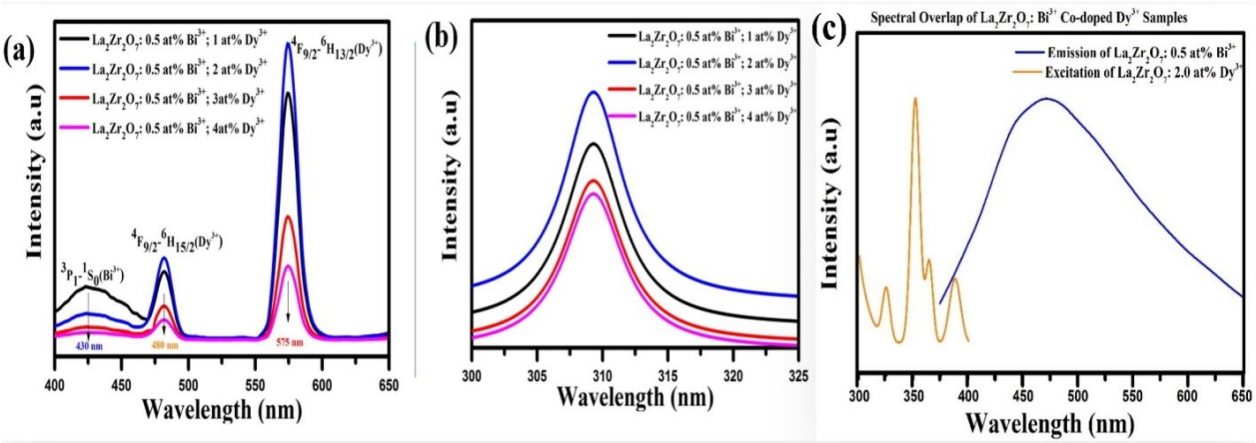

Fig. 5. Photoluminescence (a) Emission spectra (λ_{ex} = 330 nm), (b) Excitation spectra (λ_{em} = 575 nm) of Bi^{3+}/Dy^{3+} co-doped $La_2Zr_2O_7$ nanophosphors and (c) Spectral overlap of excitation spectrum (λ_{em} = 575 nm) of $La_2Zr_2O_7$: 2 at%. $Dy^{3+}$and emission spectrum of $La_2Zr_2O_7$: 0.5 at. % Bi^{3+} (λ_{ex} = 330 nm).

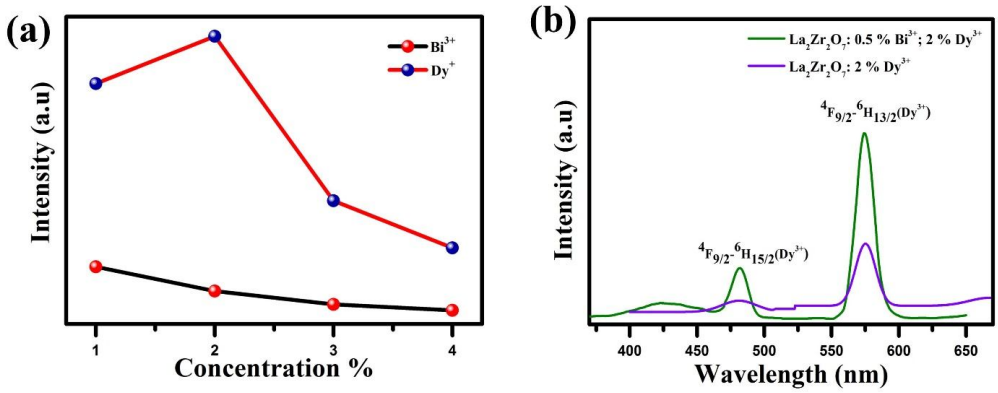

Fig. 6. (a) Intensity variation of Bi^{3+} as a function of Dy^{3+} and (b) Comparison of singly doped Dy^{3+} (Ex at 285 nm) and Bi^{3+}/ Dy^{3+} co-doped $La_2Zr_2O_7$.

Furthermore, from the excitation spectra of the Bi^{3+}/Dy^{3+} co-doped nanophosphor samples, it was monitored that at 575 nm ($^4F_{9/2}$-$^6H_{13/2}$) of Dy^{3+} ions, the broad peak in the range of 300-330 nm of Bi^{3+} (Fig. 4b) and the charge transfer absorption band peak of Dy^{3+} centred at 307 nm (Fig. 5b) overlapped with virtue of Bi^{3+} co-doping.

The spectral overlap between the Dy^{3+} ions emission band and the Bi^{3+} ions excitation band in the as-prepared samples is shown in Fig. 5c, which suggests the possibility of energy transfer (ET) between the energy levels of Bi^{3+} and Dy^{3+} ions [24]. This indicated that the activator Dy^{3+} was sensitized by the excited Bi^{3+} in the host lattice, demonstrating the existence of an efficient energy transfer (ET) from the Bi^{3+} ions to the Dy^{3+} ions [25]. Figure 6a shows the intensity variation in emission spectra of Bi^{3+} ions as a function of Dy^{3+} ions concentration, and Fig. 6b shows the singly doped $La_2Zr_2O_7$: 2 at% Dy^{3+}emission spectra (violet) and the Bi^{3+}/ Dy^{3+} co-doped $La_2Zr_2O_7$ (green).

Energy Transfer (ET) Mechanism in Bi^{3+}/Dy^{3+} co-doped $La_2Zr_2O_7$ Phosphors

Figure 7a illustrates the energy transfer mechanism in as-prepared samples. Under UV excitation (280-350 nm), the electrons of the Bi^{3+} ions absorbed energy and excited to a higher excited state $^3P_1$, and then relaxed to the lower energy level (the bottom of the parabola) by non-radiative relaxation. When de-excited from the $^3P_1$ level of Bi^{3+}, energy can be transferred through the ET (cross relaxation) process to the $^4G_{11/2}$ level of Dy^{3+}. Some electrons of Bi^{3+} ions might radiate back to the ground state by emitting blue (~430 nm) emission that could be reabsorbed by the Dy^{3+} ground state levels; $^6H_{15/2}$ resulted in energy transfer (due to spectral overlap) and was excited to the relative excited states. The excited electrons further relaxed to the $^4F_{9/2}$ level of Dy^{3+} through a non-radiative transition, and then de-excited to the $^4F_{9/2}$-$^6H_{15/2}$ and $^6H_{11/2}$ levels of Dy^{3+}ions by emitting blue (~480 nm) and strong yellow (~575 nm) lines, respectively [26-28].

The CIE chromaticity coordinates of 0.5 at% Bi^{3+} and Bi^{3+}/Dy^{3+} co-doped $La_2Zr_2O_7$ are shown in Fig. 7b and Table 3. From Fig. 7b, the hue of the as-prepared samples can be tuned from blue → cyan → yellow when co-doping the host sample with Bi^{3+}/Dy^{3+}. Finally, the enhanced luminescence intensity observed from Fig. 6b, and the ET and CIE observed from Figs. 7a and b indicate that the as-prepared phosphor may potentially be used as a single-phase phosphor for pc-LED and field display device applications.

Table 3. CIE Chromatic Co-ordinates, CCT and Colour Purity of Bi^{3+}/Dy^{3+} co-doped $La_2Zr_2O_7$ Nanophosphors

Phosphor	Symbol	X	Y	CCT	Purity
1 at.% Dy^{3+}	A	0.28	0.28	10619	23.3
2 at.% Dy^{3+}	B	0.39	0.4.0	3922	37.4
3 at.% Dy^{3+}	C	0.37	0.38	4315	25.2
4 at.% Dy^{3+}	D	0.32	0.34	6072	4.20
0.5 at.% Bi^{3+}	α	0.27	0.30	10477	22.6

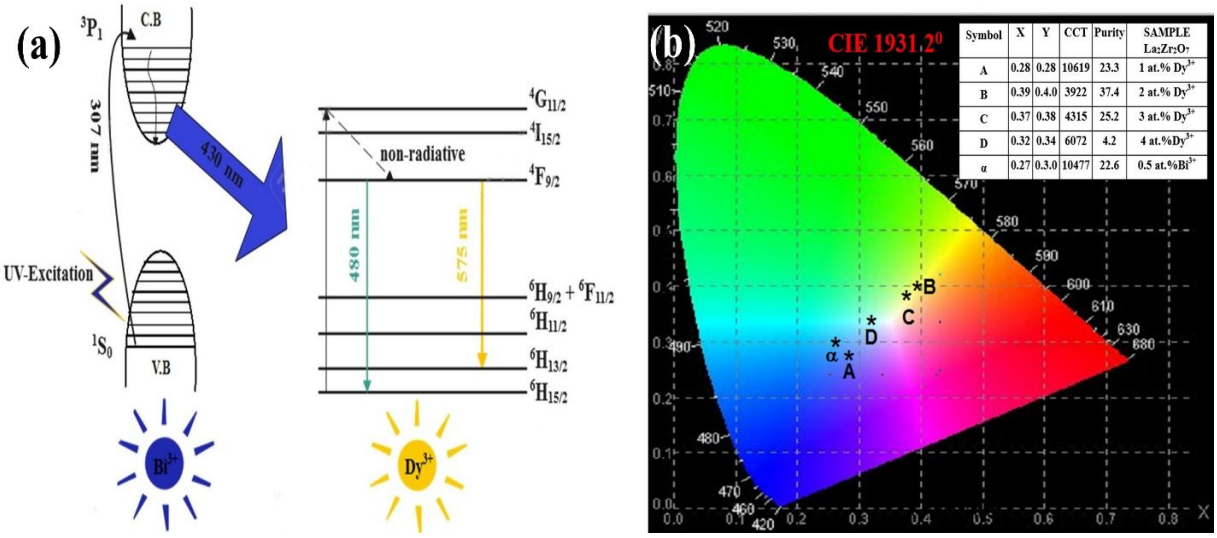

Fig. 7. (a) Energy Transfer diagram and (b) CIE chromaticity diagram of Bi^{3+}/Dy^{3+} co-doped $La_2Zr_2O_7$ nanophosphors.

CONCLUSIONS

A series of Bi^{3+} and Dy^{3+} co-doped $La_2Zr_2O_7$ nanophosphors were prepared using the polyol method. The optimized composition among the prepared nanophosphors was $La_2Zr_2O_7$: 0.5 at% Bi^{3+}; 2 at% Dy^{3+}. From the UV-Vis absorption studies, the prepared samples were capable of absorbing UV energy. The luminescent properties of the Bi^{3+}/Dy^{3+} co-doped $La_2Zr_2O_7$ nanophosphors, and energy transfer from sensitizer (Bi^{3+}) to activator (Dy^{3+}) were studied. The measured Bi-exponential life-time values of the $La_2Zr_2O_7$:Bi^{3+} (0.1, 0.5, 1, & 1.5 at.%) were correlated with the dopant concentration. In the co-doped sample, Bi^{3+} ions emitted a broad peak at ~430 nm (blue), which was attributed to the transition from $^3P_1 \rightarrow {}^1S_0$. The Dy^{3+} ions emitted broad peaks at ~480 nm (blue) and ~575 nm (yellow), which were attributed to $^4F_{9/2} \rightarrow {}^6H_{15/2}$ and $^6H_{11/2}$, respectively. The remarkable enhancement of Dy^{3+} emission by Bi^{3+} co-doping, and tunable emissions from CIE coordinates make the Bi^{3+}/Dy^{3+} co-doped $La_2Zr_2O_7$ nanophosphors a promising material that can be used in pc-LED and display applications.

ACKNOWLEDGEMENTS

Authors are thankful to Dr. David Kumar Rapaka, Principal, Government College (A), Rajahmundry for permitting to perform experiments in Crystal Growth and Nano Science Research Centre. Authors are grateful to Dr. Y.S. Chaudhary, CSIR-IMMT, Bhubaneswar for providing permission to explore photoluminescence studies and one of the authors (B.V. Naveen Kumar) would thank the HoD, Principal and Management of Shri Vishnu Engineering College for Women (Autonomous), Bhimavaram for their continuous support and encouragement.

REFERENCES

[1] Tsang, M. -K.; Bai, G.; Hao, J., Stimuli responsive upconversion luminescence nanomaterials and films for various applications. *Chem. Soc. Rev.* **2015**, *44*, 1585-1607. http://dx.doi.org/10.1039/C4CS00171K.

[2] Tian, L.; Shen, J.; Xu, T.; Wang, L.; Zhang, L.; Zhang, J.; Zhang, Q., Dy^{3+} doped thermally stable garnet-based phosphors: luminescence improvement by changing the host-lattice composition and co-doping Bi^{3+}. *RSC Adv.* **2016**, *6*, 32381-32388. https://doi.org/10.1039/C6RA04761K.

[3] Lai, S.; Yang, Z.; Liao, J.; Qiu, J.; Song, Z.; Yang, Y.; Zhou, D., Investigation of persistent luminescence property of Bi^{3+}, Dy^{3+} co-doped $CdSiO_3$ phosphor. *Mater. Res. Bull.* **2014**, *60*, 714-718.

https://doi.org/10.1016/j.materresbull.2014.09.049.

[4] Zhang, W.; Liu, S.; Hu, Z.; Liang, Y.; Feng, Z.; Sheng, X., Preparation of YBO_3:Dy^{3+}, Bi^{3+} phosphors and enhanced photoluminescence. *Mater. Sci. Engin. B* **2014**, *187*, 108-112. https://doi.org/10.1016/j.mseb.2014.05.006.

[5] Tian, L.; Wang, L.; Zhang, L.; Zhang, Q.; Ding, W.; Yu, M., Enhanced luminescence of Dy^{3+}/Bi^{3+} co-doped $Gd_3Al_5O_{12}$ phosphors by high-efficiency energy transfer. *J. Mater. Sci.: Materials in Electronics* **2015**, *26*, 8507-8514. https://doi.org/10.1007/s10854-015-3522-1.

[6] Lakshminarasimhan, N.; Varadaraju, U. V., Luminescent host lattices, LaInO3 and $LaGaO_3$-A reinvestigation of luminescence of d10 metal ions. *Mater. Res. Bull.* **2006**, *41*, 724-731. https://doi.org/10.1016/j.materresbull.2005.10.010.

[7] Abdou, M.; Gupta, S. K.; Zuniga, J. P.; Mao, Y., On structure and phase transformation of uranium doped $La_2Hf_2O_7$ nanoparticles as an efficient nuclear waste host. *Mater. Chem. Front.* **2018**, *2*, 2201-2211. http://dx.doi.org/10.1039/C8QM00266E.

[8] Gupta, S. K.; Abdou, M.; Ghosh, P. S.; Zuniga, J. P.; Mao, Y., Thermally induced disorder-order phase transition of $Gd_2Hf_2O_7$:Eu^{3+} nanoparticles and its implication on photo- and radioluminescence. *ACS Omega* **2019**, *4*, 2779-2791. https://doi.org/10.1021/acsomega.8b03458.

[9] Sakharov, K. A.; Simonenko, E. P.; Simonenko, N. P.; Vaganova, M. L.; Lebedeva, Y. E.; Chaynikova, A. S.; Osin, I. V.; Sorokin, O. Y.; Grashchenkov, D. V.; Sevastyanov, V. G., *et al.* Glycol-citrate synthesis of fine-grained oxides La^{2-}xGdxZr_2O_7 and preparation of corresponding ceramics using FAST/SPS process. *Ceram. Int.* **2018**, *44*, 7647-7655. https://doi.org/10.1016/j.ceramint.2018.01.188.

[10] Guo, C.; Ding, X.; Luan, L.; Xu, Y., Two-color emitting of Eu^{2+} and Mn^{2+} co-doped $Sr_2Mg_3P_4O_{15}$ for UV LEDs. *Sens. Actuators B: Chem.* **2010**, *143*, 712-715. https://doi.org/10.1016/j.snb.2009.10.023.

[11] Xie, M.; Li, D.; Pan, R.; Zhou, X.; Zhu, G., Crystallographic sites of Eu^{2+} and Eu^{2+}-Tb^{3+} energy transfer in Sr_2LiSiO_4F. *RSC Adv.* **2015**, *5*, 22856-22862. http://dx.doi.org/10.1039/C5RA00585J.

[12] Park, S. Ce^{3+}-Mn^{2+} cooperative $Ba_9Y_2Si_6O_{24}$ orthosilicate phosphors. *Mater. Lett.* **2014**, *135*, 59-62. https://doi.org/10.1016/j.matlet.2014.07.134.

[13] Lee, S.; Park, S., Preparation and luminescent properties of Tb^{3+} and Tb^{3+}-Ce^{3+} doped $Ba_9Y_2Si_6O_{24}$ phosphors. *J. Lumin.* **2013**, *143*, 215-218. https://doi.org/10.1016/j.jlumin.2013.05.008.

[14] Tian, L.; Shen, J.; Xu, T.; Wang, L.; Zhang, L.; Zhang, J.; Zhang, Q., Dy^{3+} doped thermally stable garnet-based phosphors: luminescence improvement by changing the host-lattice composition and co-doping Bi^{3+}. *RSC Adv.* **2016**, *6*, 32381-32388. DOI: https://doi.org/10.1039/C6RA04761K.

[15] Li, K.; Lian, H.; Shang, M.; Lin, J., A novel greenish yellow-orange red $Ba_3Y_4O_9$:Bi^{3+}, Eu^{3+} phosphor with efficient energy transfer for UV-LEDs. *Dalton Trans.* **2015**, *44*, 20542-20550. http://dx.doi.org/10.1039/C5DT03565A.

[16] Sun, Z.; Wang, M.; Yang, Z.; Jiang, Z.; Liu, K.; Ye, Z., Enhanced red emission from Eu^{3+}-Bi^{3+} co-doped Ca_2YSbO_6 phosphors for white light-emitting diode. *J. Alloys Compd.* **2016**, *658*, 453-458. https://doi.org/10.1016/j.jallcom.2015.10.242.

[17] Pokhrel, M.; Alcoutlabi, M.; Mao, Y., Optical and X-ray induced luminescence from Eu^{3+} doped $La_2Zr_2O_7$ nanoparticles. *J. Alloys Compd.* **2017**, *693*, 719-729. https://doi.org/10.1016/j.jallcom.2016.09.218.

[18] Chawla, A. K.; Kaur, D.; Chandra, R., Structural and optical characterization of ZnO nanocrystalline films deposited by sputtering. *Opt. Mater.* **2007**, *29*, 995-998. https://doi.org/10.1016/j.optmat.2006.02.020.

[19] Siwach, A.; Kumar, D., Structural and optical behavior of nano-scaled luminous green-emitting $Ca_9Y(PO_4)7$:Tb^{3+} phosphor for competent lighting devices. *Chem. Phys. Lett.* **2021**, *772*, 138547. https://doi.org/10.1016/j.cplett.2021.138547.

[20] Jamil, H.; Dildar, I. M.; Ilyas, U.; Hashmi, J. Z.; Shaukat, S.; Sarwar, M. N.; Khaleeq-ur-Rahman, M., Microstructural and optical study of polycrystalline manganese oxide films using Kubelka-Munk function. *Thin Solid Films* **2021**, *732*, 138796. https://doi.org/10.1016/j.tsf.2021.138796.

[21] Lavanya, D. R.; Darshan, G. P.; Malleshappa, J.; Premkumar, H. B.; Sharma, S. C.; Hariprasad, S. A.;

Nagabhushana, H., Enrichment of luminescence *via* incorporation of fluxes in $La_2Zr_2O_7:Tb^{3+}$ nanophosphors: One material, many possibilities-latent fingerprint visualization, Anti- counterfeiting, luminescent flexible films. *Sci. Rep.* **2022**, *1*, 1-34. https://doi.org/10.21203/rs.3.rs-1158151/v1.

[22] Talari, S.; Chirauri, S. K.; Reddy, P. V. S. S. S. N.; Rao, K. R., Photoluminescence studies of Bi^{3+}/Dy^{3+} co-doped $LaGaO_3$ nanophosphors for display device applications. *Mater. Today: Proc.* **2021**, *52*, 2224-2227. https://doi.org/10.1016/j.matpr.2021.08.042.

[23] Dutta, S.; Som, S.; Sharma, S. K., Luminescence and photometric characterization of K^+ compensated $CaMoO_4:Dy^{3+}$ nanophosphors. *Dalton Trans.* **2013**, *42*, 9654-9661. http://dx.doi.org/10.1039/C3DT50780G.

[24] Wu, H.; Li, H.; Jiang, L.; Tan, T.; Wang, S.; Jiao, S.; Yuan, W.; Su, J.; Li, C.; Zhang, H., Design of white-emitting optical temperature sensor based on energy transfer in a Bi^{3+}, Eu^{3+} and Tb^{3+} doped YBO_3 crystal. *J. Mater. Chem. C* **2021**, *9*, 7264-7273. http://dx.doi.org/10.1039/D1TC01585K.

[25] Hussain, S. K.; Bharat, L. K.; Kim, D. H.; Yu, J. S., Facile pechini synthesis of $Sr_3Y_2Ge_3O_{12}:Bi^{3+}/Eu^{3+}$ phosphors with tunable emissions and energy transfer for WLEDs. *J. Alloys Compd.* **2017**, *703*, 361-369. https://doi.org/10.1016/j.jallcom.2017.01.345.

[26] Perumal, R. N.; Lopez, A. X.; Subalakshmi, G., Synthesis and luminescence property of Bi^{3+} and Dy^{3+} ions doped MLa_2O_4 (M = Ba, Sr and Ca) phosphors for LEDs application. *Optik* **2019**, *179*, 1001-1008. https://doi.org/10.1016/j.ijleo.2018.09.173.

[27] Mu, Z.; Hu, Y.; Chen, L.; Wang, X., Enhanced luminescence of Dy^{3+} in $Y_3Al_5O_{12}$ by Bi^{3+} co-doping. *J. Lumin.* **2011**, *131*, 1687-1691. https://doi.org/10.1016/j.jlumin.2011.03.072.

[28] He, H.; Fu, R.; Cao, Y.; Song, X.; Pan, Z.; Zhao, X.; Xiao, Q.; Li, R.. $Ce^{3+}\rightarrow Eu^{2+}$ energy transfer mechanism in the $Li_2SrSiO_4:Eu^{2+}$, Ce^{3+} phosphor. *Opt. Mater.* **2010**, *32*, 632-636. https://doi.org/10.1016/j.optmat.2010.01.009.